Electronic Supplementary Information

Experimental section

Materials: Nickel foam (NF) was provided by Hongshan District, Wuhan Instrument Surgical Instruments business, and treated in hydrochloric acid (HCl) to serve as substrate for active materials. $FeCl_3 \cdot 6H_2O$, terephthalic acid (HCl) and N, N-dimethylformamide (DMF) were purchased from Aladdin Ltd. in Shanghai. C_2H_5OH was purchased by Chengdu Kelon Chemical Reagent Factory. All chemical regents were used as received without further purification. The water used throughout all experiments was purified through a Millipore system.

Preparation of Fe-MOF/NF: Fe-MOF/NF was prepared as follows. A piece of NF was first treated with concentrated HCl, ethanol and deionized water by sonication sequentially to obtain a clean surface before use. To prepare Fe-MOF/NF using a hydrothermal reaction, 1 mmol $FeCl_3 \cdot 6H_2O$ (0.2703 g) and 1 mmol terephthalic acid (0.166 g) were dissolved in 35 mL DMF to form a solution. 2.5 mL ethanol and 2.5 mL distilled water were added slowly to the solution under constant stirring. Then the solution was transferred to a 50 mL Teflon-lined stainless-steel autoclave in which a piece of NF was immersed into the solution. The autoclave was sealed and maintained at 125 °C for 12 h in an electric oven to obtain Fe-MOF/NF. After the autoclave cooled down naturally, the Fe-MOF/NF was taken out and washed with water and ethanol for several times, followed by drying 2 h at 60 ºC.

Synthesis of RuO_2: RuO_2 was prepared in accordance with reported work.[1] Briefly, 2.61 g of $RuCl_3 \cdot 3H_2O$ and 1.0 mL KOH (1.0 M) were added into 100 mL distilled water and stirred for 45 min at 100 °C. Then the above solution was centrifuged for 10 min and filtered. The precipitates were collected by centrifugation and washed with water for several times, followed by drying at 70 °C. Finally, the product was annealed at 300 °C for 3 h under air atmosphere. RuO_2 ink was prepared by dispersing 20 mg of catalyst into 490 μL of water/ethanol (v/v = 1:1) and 10 μL of 5 wt% Nafion using sonication for 30 min. Then 29.5 μL of the RuO_2 ink (containing 1.475 mg of RuO_2) was loaded onto a bare NF of 0.25 cm^{-2} in geometric area (loading:

5.9 mg cm^{-2}).

Characterizations: Transmission electron microscopy (TEM) images were collected on a HITACHI H-8100 electron microscopy (Hitachi, Tokyo, Japan) operated at 200 kV. Scanning electron microscopy (SEM) measurements were performed on a XL30 ESEM FEG scanning electron microscope at an accelerating voltage of 20 kV. X-ray photoelectron spectroscopy (XPS) spectra were acquired on an ESCALABMK II X-ray photoelectron spectrometer using Mg as the exciting source.

Electrochemical measurements: Electrochemical measurements were performed with a CHI 660E electrochemical analyzer (CH Instruments, Inc., Shanghai) in a standard three-electrode system using a Fe-MOF/NF as the working electrode, a graphite plate as the counter electrode and Hg/HgO as the reference electrode. The potentials reported in this work were calibrated to RHE, using the following equation: E (RHE) = E (Hg/HgO) + (0.098 + 0.059 pH) V. Polarization curves were obtained by linear sweep voltammetry with a scan rate of 5 mV s^{-1}. All experiments were carried out at room temperature (~25 °C).

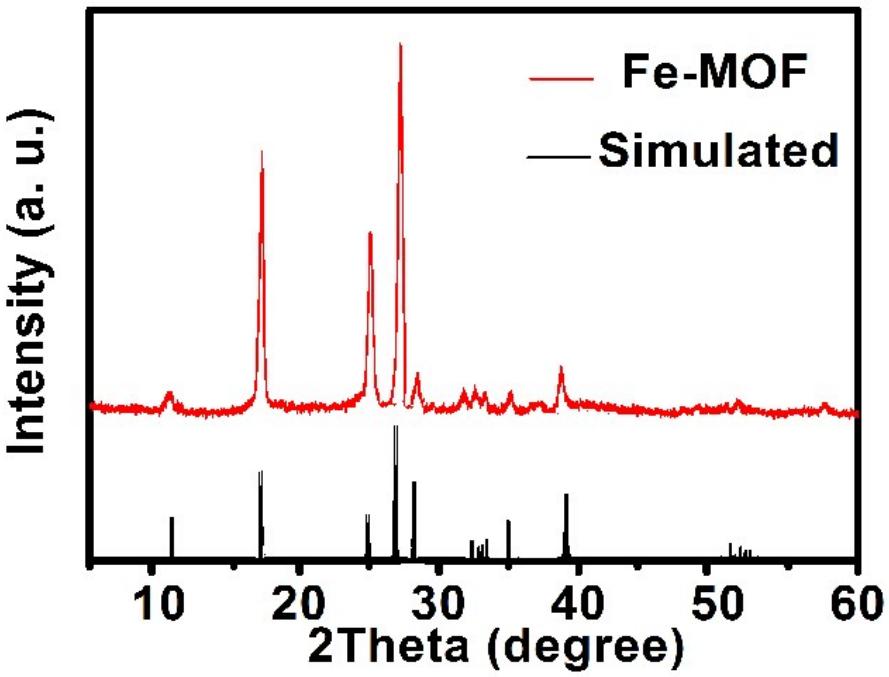

Fig. S1. XRD pattern for Fe-MOF powder.

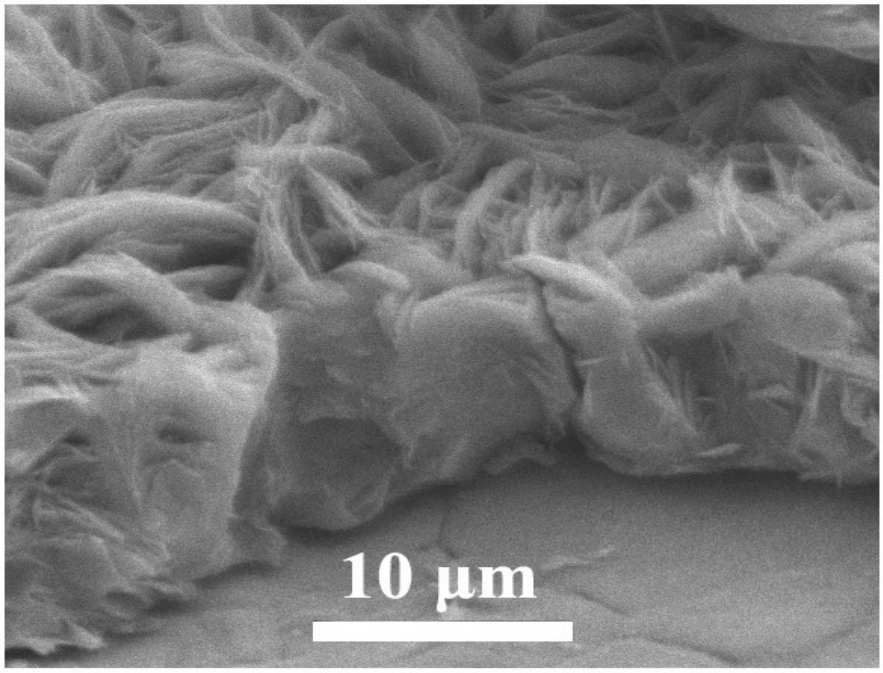

Fig. S2. Cross-section SEM image of Fe-MOF/NF.

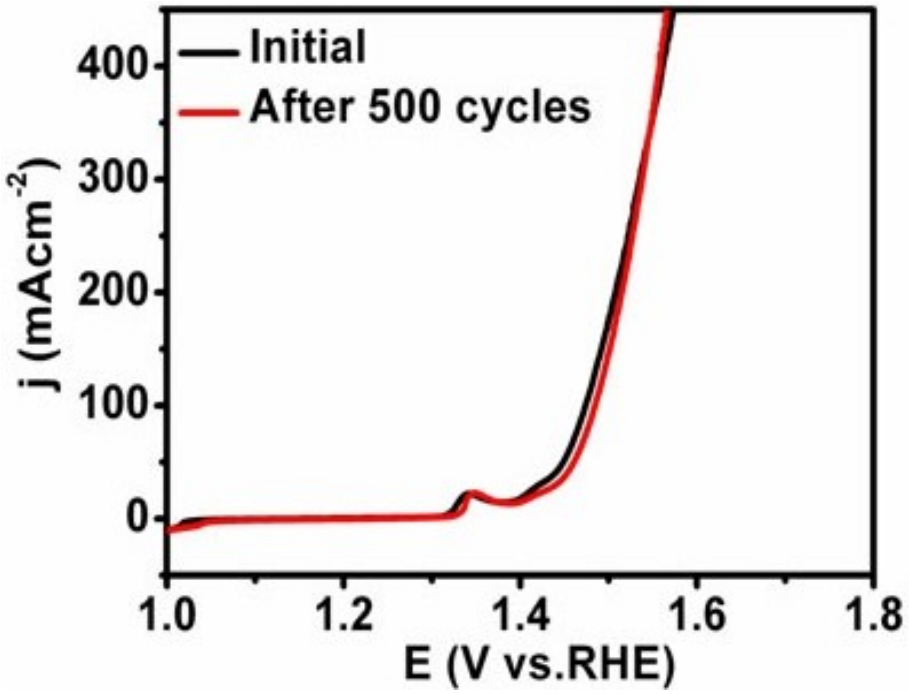

Fig. S3. LSV curves recorded of Fe-MOF/NF before and after 500 CV cycles in 1.0 M KOH.

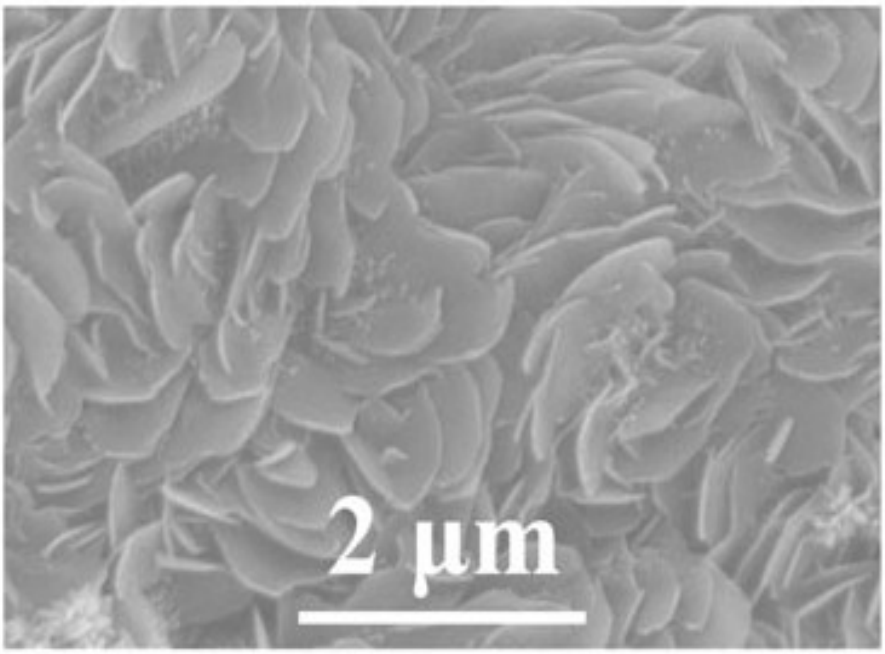

Fig. S4. SEM image of Fe-MOF/NF after stability test.

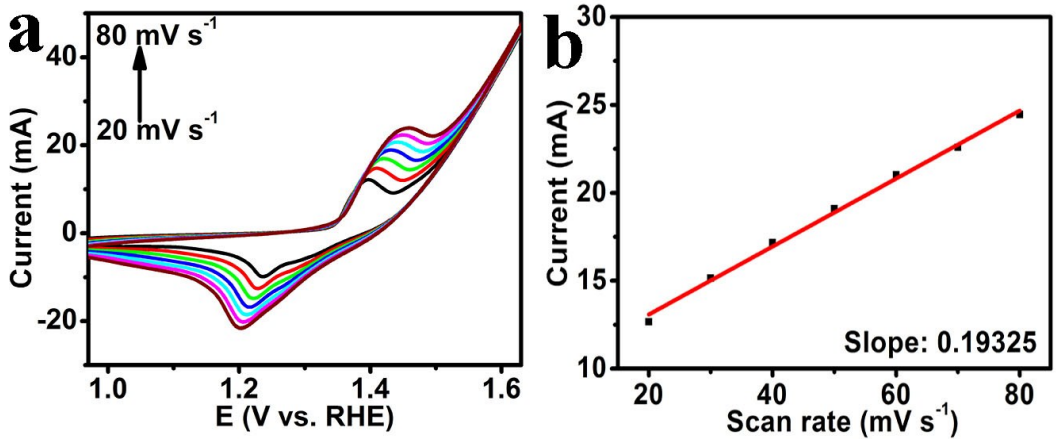

Fig. S5. (a) CVs of Fe-MOF/NF under different scan rates increasing from 20 to 80 mV s^{-1} in 1.0 M KOH. (b) Linear relationship of the oxidation peak currents vs. scan rates for Fe-MOF/NF.

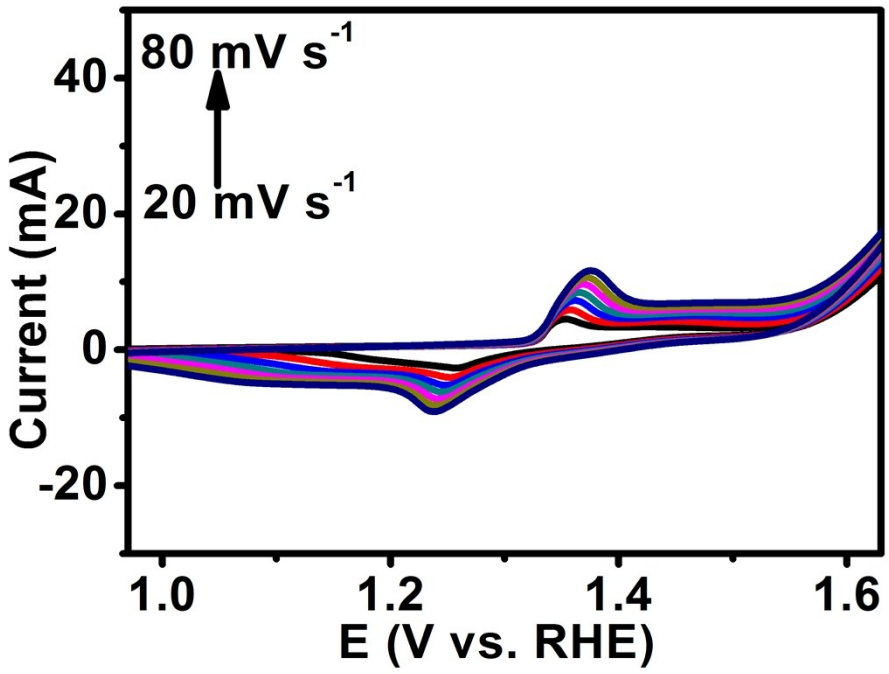

Fig. S6. CVs of Ni foam under different scan rates increasing from 20 to 80 mV s^{-1} in 1.0 M KOH.

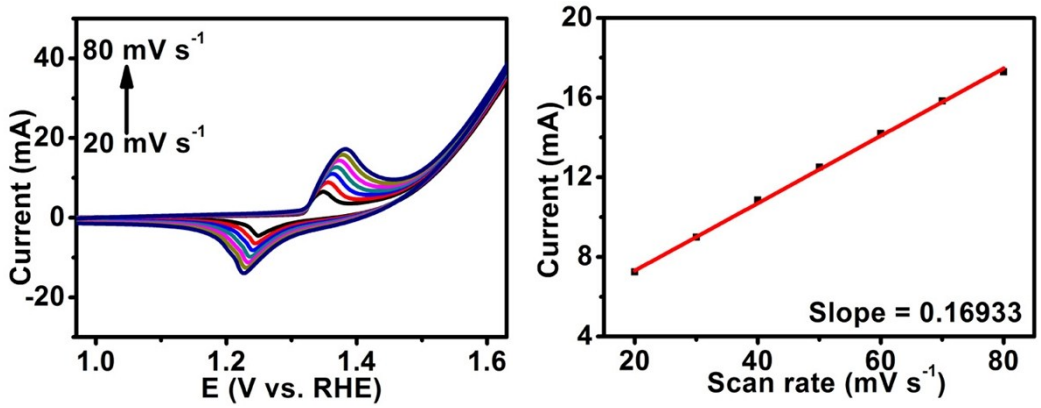

Fig. S7 (a) CVs of RuO_2/NF different scan rates increasing from 20 to 80 mV s^{-1} in 1.0 M KOH. (b) Linear relationship of the oxidation peak currents vs. scan rates for RuO_2/NF.

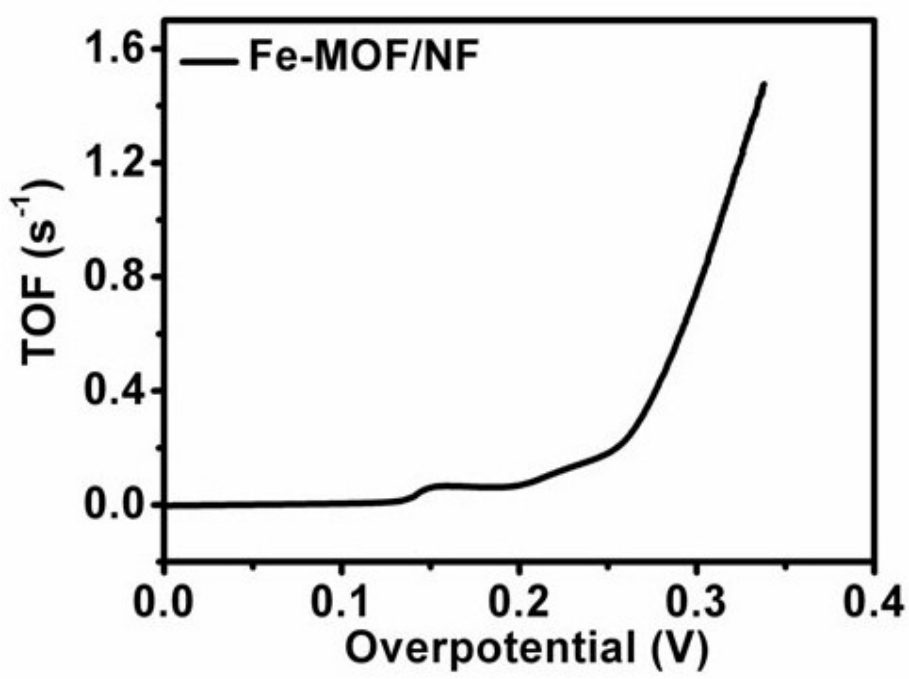

Fig. S8. Plot of TOF vs. overpotential for Fe-MOF/NF.

Table S1. Comparison of the OER activity for Fe-MOF/NF with other non-noble-metal electrocatalysts in alkaline media.

Catalyst	j ($mA\ cm^{-2}$)	η (mV)	Electrolyte	Ref.
Fe-MOF/NF	50	240	1.0 M KOH	This work
Fe_xN	50	270	1.0 M KOH	2
iron oxide	10	339	1.0 M KOH	2
Iron Phosphide Nanotubes	20	300	1.0 M KOH	3
$Fe_{1.1}Mn_{0.9}P$	10	430	1.0 M KOH	4
FeP@Au	10	320	1.0 M KOH	5
$(Co_{0.54}Fe_{0.46})_2P$	10	370	1.0 M KOH	6
FeS_x	10	420	0.1 M KOH	7
iron oxyhydroxide	20	510	1.0 M NaOH	8
Ni_2P nanoparticles	10	290	1.0 M KOH	9
CoNi SUNOE	10	450	1.0 M KOH	10
Fe-Ni oxide	10	>375	1.0 M KOH	11
NiCo LDH	10	367	1.0 M KOH	12
NiOOH	10	525	1.0 M KOH	13
NiFe LDH/NF	10	269	1.0 M KOH	14
NiFe-NS	10	300	1.0 M KOH	15
NiFe-LDH/CNT	10	250	1.0 M KOH	16
Co-P film	10	345	1.0 M KOH	17
Co-Ni-Fe_{511}	10	288	1.0 M KOH	18
Ni-Fe (oxy) hydroxide	10	275	1.0 M KOH	19

References

1 J. C. Cruz, V. Baglio, S. Siracusano, V. Antonucci, A. S. Aricò, R. Ornelas, L. Ortiz-Frade, G. Osorio-Monreal, S. M. Durón-Torres and L. G. Arriaga, *Int. J. Electrochem. Sci.*, 2011, **6**, 6607–6619.

2 F. Yu, H. Zhou, Z. Zhu, J. Sun, R. He, J. Bao, S. Chen and Z. Ren, *ACS Catal.*, 2017, **7**, 2052–2057.

3 Y. Yan, B.Xia, X. Ge, Z. Liu, A. Fisher and X. Wang, *Chem. Eur. J.*, 2015, **21**, 48062–18067.

4 D. Li, H. Baydoun, B. Kulikowski and S. L. Brock, *Chem. Mater.*, 2017, **29**, 3048–3054.

5 J. Masud, S. Umapathi, N. Ashokaan and M. Nath, *J. Mater. Chem. A*, 2016, **4**, 9750–9754.

6 E. J. Popczun, C. W. Roske, C. G. Read, J. C. Crompton, J. M. McEnaney, J. F. Callejas, N. S. Lewis and R. E. Schaak, *J. Mater. Chem. A*, 2015, **3**, 5420–5425.

7 B. C. M. Martindale and E. Reisner, *Adv. Energy Mater.*, 2016, **6**, 1502905.

8 D. R. Chowdhury, L. Spicia, S. S. Amritphale, A. Paul and A. Singh, *J. Mater. Chem. A*, 2016, **4**, 3655–3660.

9 L.-A. Stern, L. Feng, F. Song and X. Hu, *Energy Environ. Sci.*, 2015, **8**, 2347–2351.

10 B. Ni and X. Wang, *Chem. Sci.*, 2015, **6**, 3572–3576.

11 J. Landon, E. Demeter, N. İnoğlu, C. Keturakis, I. E. Wachs, R. Vasić, A. I. Frenkel and J. R. Kitchin, *ACS Catal*., 2012, **2,** 1793–1801.

12 H. Liang, F. Meng, M. Cabán-Acevedo, L. Li, A. Forticaux, L. Xiu, Z. Wang and S. Jin, *Nano Lett.*, 2015, **15**, 1421–1427.

13 S. Klaus, Y. Cai, M. W. Louie, L. Trotochaud and A. T. Bell, *J. Phys. Chem. C*, 2015, **119**, 7243–7254.

14 J. Luo, J.-H. Im, M. T. Mayer, M. Schreier, M. K. Nazeeruddin, N.-G. Park, S. D. Tilley, H. Fan and M. Graetzel, *Science*, 2014, **345**, 1593–1596.

15 F. Song and X. Hu, *Nat. Commun.*, 2014, **5**, 4477.

16 M. Gong, Y. Li, H. Wang, Y. Liang, J. Z. Wu, J. Zhou, J. Wang, T. Regier, F. Wei and H. Dai, *J. Am. Chem. Soc.*, 2013, **135**, 8452–8455.

17 N. Jiang, B. You, M. Sheng and Y. Sun, *Angew. Chem., Int. Ed.*, 2015, **54**, 6251–6254.

18 G. Zeng, M. Liao, C. Zhou, X. Chen, Y. Wang and D. Xiao, *RSC Adv.*, 2016, **6**, 42255–42262.

19 A. S. Batchellor and S. W. Boettcher, *ACS Catal*., 2015, **5**, 6680–6689.